

# Preparation and Characterization of 3,3',4,4'-Benzophenone Tetracarboxylic Dianhydride–Pyromellitic Dianhydride Alternating Polyimides

YU YANG,\* XUJIE YANG, ZHENGLIANG ZHI, LUDE LU, XIN WANG

Materials Chemistry Laboratory, Nanjing University of Science and Technology, Nanjing 210094, People's Republic of China

Received 20 May 1996; accepted 23 September 1996

**ABSTRACT:** Four kinds of 3,3',4,4'-benzophenone tetracarboxylic dianhydride (BTDA)–pyromellitic dianhydride (PMDA) alternating polyimide (BTDA–PMDA API) were obtained by reacting 1 mol BTDA with 2 mol diamines to form BTDA chain-extended diamines (BTDA CED), followed by the addition of 1 mol PMDA to yield the BTDA–PMDA alternating polyamic acids (BTDA–PMDA APA), and finally by imidizing them thermally. BTDA CED were characterized by elemental analysis, infrared (IR), and <sup>1</sup>H-NMR spectroscopy. The structures of BTDA–PMDA APA and BTDA–PMDA API were investigated by IR and <sup>1</sup>H-NMR spectroscopy, and their thermal properties and interfacial tension were also studied. Furthermore, the characteristic properties of BTDA–PMDA API were compared with their corresponding homopolyimides from BTDA (BTDA HPI) and from PMDA (PMDA HPI). It was found that the alternating condensation polymerization is an effective method to modify polyimides interfacial tension with a small influence on the thermal stability. © 1997 John Wiley & Sons, Inc. *J Appl Polym Sci* **64**: 1585–1593, 1997

**Key words:** preparation; characterization; 3,3',4,4'-benzophenone tetracarboxylic dianhydride; pyromellitic dianhydride; polyimide

## INTRODUCTION

Polyimides were first prepared by Bogert and Renshaw<sup>1</sup> in 1908, and they were then widely used and rapidly developed because of their outstanding characteristics of good tractability, high thermal stability, great mechanical stability, good water resistance, grind resistance, fire and radiation resistance, and relatively low cost. For practical purposes, much work, which may be classified

into two aspects, has been done to modify the polyimides. One is to introduce such groups as amide,<sup>2</sup> sulfone,<sup>3</sup> ether,<sup>4</sup> among others, into the chains; our recent work in the preparation of polyimides with metals in the main chain has been reported.<sup>5,6</sup> The other is to react no less than two diamines with a dianhydride, or vice versa, to get alternating polyimides.<sup>7</sup> According to Adrova et al.,<sup>8</sup> cocondensed polyimides are superior to their corresponding homopolyimides in regard to mechanical and thermal properties, as well as adhesive strength with metals and glass.

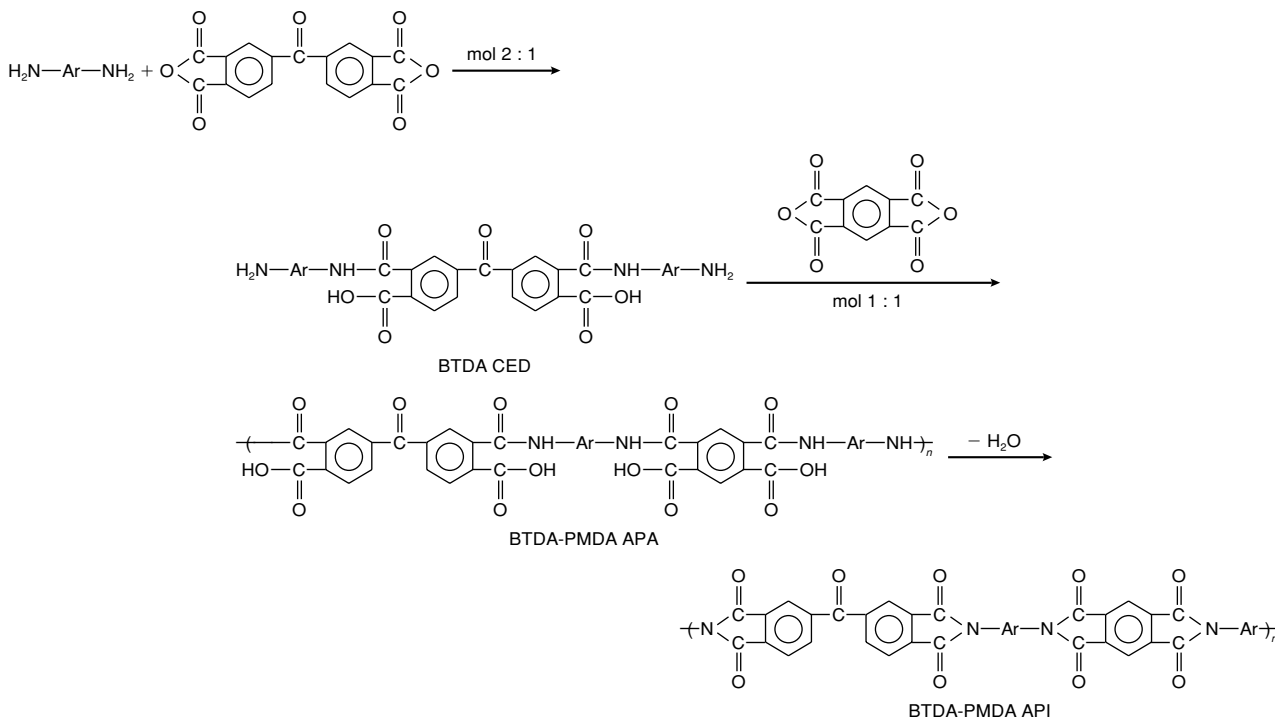
Strictly alternating copolyimides from two different dianhydrides and one aliphatic spacer prepared by the reaction of imide containing diisocyanates with different dianhydrides have been reported by Avadhani and Vernekar.<sup>9</sup> They found that these

Correspondence to: X. Wang.

\* Present address: Department of Chemistry, Nanjing University, Nanjing 210093, People's Republic of China.

Contract grant sponsor: State Education Commission of China.

© 1997 John Wiley & Sons, Inc. CCC 0021-8995/97/081585-09



Scheme 1

polyimides had very good solubility in many polar solvents, and the thermal stability was intermediate between the two sets of homopolyimides. Little information, however, is available concerning the surface energy of these kinds of polymers. In the present investigation, a series of 3,3',4,4'-benzophenone tetracarboxylic dianhydride (BTDA)-pyromellitic dianhydride (PMDA) alternating polyimide (BTDA-PMDA API) were synthesized and characterized; their thermal properties, interfacial tension, and infrared (IR) and  $^1\text{H-NMR}$  spectra were studied and compared with their corresponding homopolyimides.

## EXPERIMENTAL

### Materials and Instrumentation

*N,N'*-dimethyl formamide (DMF), *p*-phenyl diamine, 4,4'-diamino dibenzene, 4,4'-diaminodiphenyl methane, and 4,4'-diaminodiphenyl ether were of analytical grade. PMDA and BTDA were the products of the Shanghai Chemical Reagents Company. IR spectra were recorded with a Shanghai 7400 IR instrument.  $^1\text{H-NMR}$  spectra were measured by a Varian FT-80A Spectrometer in  $\text{DMSO-d}_6$ . Viscosities were determined at 25°C

with a Sansei viscometer. Thermogravimetry-differential thermal analysis (TG-DTA) data were obtained by using a Beijing PCT-1 analyzer at a heating rate of 10°C min $^{-1}$  in air. For interfacial tension, contact angles were measured with a JY-80 contact angle meter.

### Synthesis of BTDA-PMDA API

Four BTDA-PMDA API were synthesized by using four diamines according to Scheme 1. Diamines may be *p*-phenyl diamine, 4,4'-diamino dibenzene, 4,4'-diaminodiphenyl methane, and 4,4'-diaminodiphenyl ether, being numbered by 1, 2, 3, and 4, respectively. Thus, results of the

**Table I** Imidization Temperatures (°C)

| Sample         | T1  | T2  | T3  |
|----------------|-----|-----|-----|
| BTDA-PMDA APA1 | 147 | 168 | 221 |
| BTDA-PMDA APA2 | 130 | 165 | 213 |
| BTDA-PMDA APA3 | 135 | 160 | 210 |
| BTDA-PMDA APA4 | 145 | 165 | 225 |

T1 and T3 are the initial and end temperatures, respectively, of weight loss in the second stage of TG curve; T2 is the temperature of the second endothermic peak in DTA curve, related to the imidization.

**Table II Elemental Analysis Data of BTDA CED (Calcd) (%)**

| Sample    | C             | H           | N           |
|-----------|---------------|-------------|-------------|
| BTDA CED1 | 64.15 (64.19) | 3.23 (3.26) | 6.50 (6.51) |
| BTDA CED2 | 64.73 (64.77) | 3.54 (3.56) | 5.48 (5.53) |
| BTDA CED3 | 69.21 (69.23) | 3.83 (3.85) | 5.30 (5.38) |
| BTDA CED4 | 66.59 (66.67) | 3.42 (3.45) | 5.31 (5.36) |

same kind from these four diamines can be denoted by the tail numbers, for example, BTDA CED1, BTDA-PMDA APA1, and BTDA-PMDA API1, etc.

The procedures for the synthesis were as follows. A flask equipped with a mechanical stirrer, thermometer, and addition funnel was filled with a solution containing 0.02 mol of diamine in 15 mL DMF. To the vigorously stirred solution, 0.01 mol BTDA dissolved in 25 mL DMF was added dropwise in 2 h. Stirring of the mixture lasted for 3 h more at ambient temperature, producing BTDA CED with a yield over 99%. Then, 0.0102 mol of PMDA powder was gradually added four times during 30 min to the solution with stirring. After 4 h of reaction, the resulting BTDA-PMDA APA was obtained. Viscosity was measured with  $\ln \eta_r/C$  to be 29.89, 32.58, 31.21, and 28.93 mL/g for BTDA-PMDA APA 1, 2, 3, and 4, respectively. The reaction solution was volatilized at room temperature for 10 h and then at 100°C *in vacuo* for 3 h; the BTDA-PMDA APA film was thus obtained. The film was heated *in vacuo* at T1, T2, and T3, originating from the TG-DTA data of BTDA-PMDA APA, as listed in Table I, for 1, 3, and 1 h, respectively, for dehydrating; and the BTDA-PMDA API film was obtained.

BTDA HPI1-4 and PMDA HPI1-4 were also

synthesized. All these homopolyimic acids have viscosities between 30 and 35 mL/g in  $\ln \eta_r/C$ .

## RESULTS AND DISCUSSION

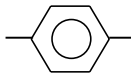
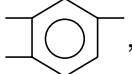
### Characterization of BTDA CED

The diamines chain-extended by BTDA were characterized by IR, <sup>1</sup>H-NMR, and elemental analysis. The results of elemental analysis of BTDA CED are shown in Table II. We can see that the experimental data agreed well with the calculated values. The characteristic absorption and assignments of BTDA CED are listed in Table III.

Figure 1 shows a typical IR spectra of BTDA

CED1, in which  $\begin{array}{c} \text{O} \\ || \\ -\text{C}-\text{OH} \end{array}$  gives the absorption bands at 2900–2720 cm<sup>-1</sup> (OH) and 1720 cm<sup>-1</sup>

$\begin{array}{c} \text{O} \\ || \\ -\text{NH}-\text{C}- \end{array}$  (C=O);  $\begin{array}{c} \text{O} \\ || \\ -\text{NH}-\text{C}- \end{array}$  exhibits absorption bands at 3400–3200 cm<sup>-1</sup> ( $\nu_{\text{NH}}$ ), 1615 CM<sup>-1</sup> ( $\nu_{\text{C=O}}$ ), 1660 cm<sup>-1</sup> ( $\nu_{\text{C-N}}$ ), and 1545 cm<sup>-1</sup> ( $\delta_{\text{C-N}}$ ); the  $-\text{NH}_2$  gives absorption bands 1620 and 3400–3200 cm<sup>-1</sup>; and the phenyl ring shows the absorption bands at 1600 and 1510 cm<sup>-1</sup>. The <sup>1</sup>H-NMR spectra of BTDA CED were recorded in DMSO-*d*<sub>6</sub> solution, and the results are listed in Table IV. Figure 2 presents the typical <sup>1</sup>H-NMR spectra of BTDA CED1, in which the peaks can be assigned as follows: the proton of  $-\text{OH}$  of carboxylic acid gave a singlet at a chemical shift of  $\delta = 10.74$  ppm, the protons in  $-\text{NH}_2$  showed one peak at  $\delta = 4.37$  ppm (exchangeable by D<sub>2</sub>O), and the peaks at  $\delta = 7.39$ –6.50 ppm and  $\delta = 8.18$ –7.67 ppm are associated with the protons of the two

phenyl rings, i.e.,  and , respectively.

**Table III Wavenumbers of BTDA CED (cm<sup>-1</sup>)**

| Sample    | $-\text{NH}_2$    | $-\text{COOH}$    | $\begin{array}{c} \text{O} \\    \\ -\text{NH}-\text{C}- \end{array}$ | Phenyl Ring  | Other Structure       |
|-----------|-------------------|-------------------|---|--------------|-----------------------|
| BTDA CED1 | 1620<br>3400–3200 | 1720<br>2900–2720 | 3400–3200, 1520<br>1615, 1660   | 1600<br>1510 |                       |
| BTDA CED2 | 1600<br>3400–3200 | 1720<br>2900–2720 | 3400–3200, 1520<br>1610, 1650   | 1600<br>1500 |                       |
| BTDA CED3 | 1610<br>3400–3200 | 1715<br>2900–2720 | 3400–3200, 1520<br>1610, 1660   | 1600<br>1500 |                       |
| BTDA CED4 | 1620<br>3400–3200 | 1730<br>2900–2720 | 3400–3200, 1510<br>1620, 1670   | 1600<br>1500 | 1250 ( $-\text{O}-$ ) |

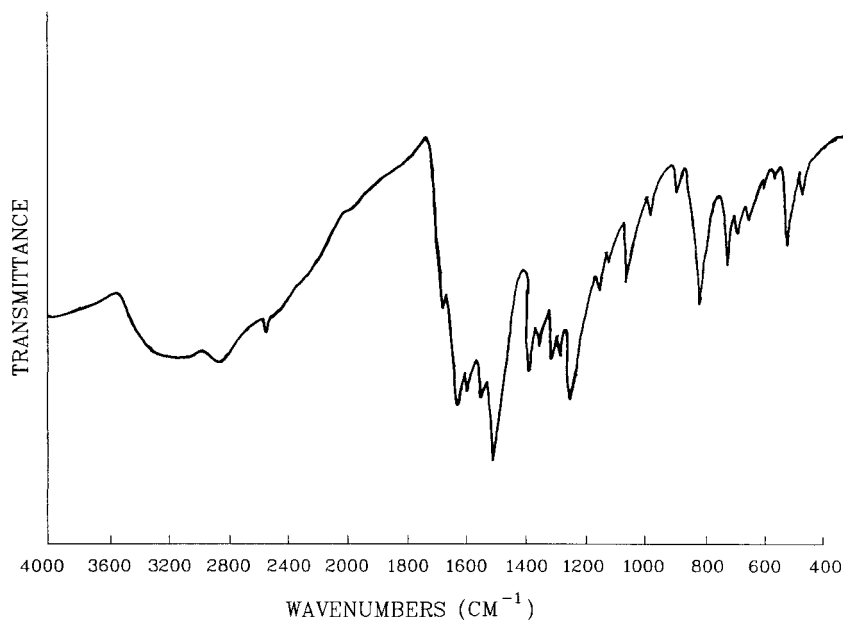



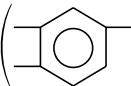
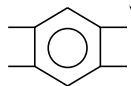
Figure 1 IR spectrum of BTDA CED1.

Based on the elemental analysis and structural characterization described above, we conclude that the BTDA CEDs have the expected structures.


#### Characterization of BTDA-PMDA API

As shown in Figure 3(a), the absorption bands of BTDA-PMDA APA1 at 3080–2700, 1710, 3380–3200, 1655, 1510, and 1315  $\text{cm}^{-1}$  are attributed to the absorption of the amic acids structure. The bands at 1510 and 1410  $\text{cm}^{-1}$  may be assigned to the phenyl ring structure. In Figure 4, the chemical shifts can be assigned as follows: 10.66

(—COOH), 7.68 (——), and 8.23–8.00

ppm (—— and ——). Also, a broad

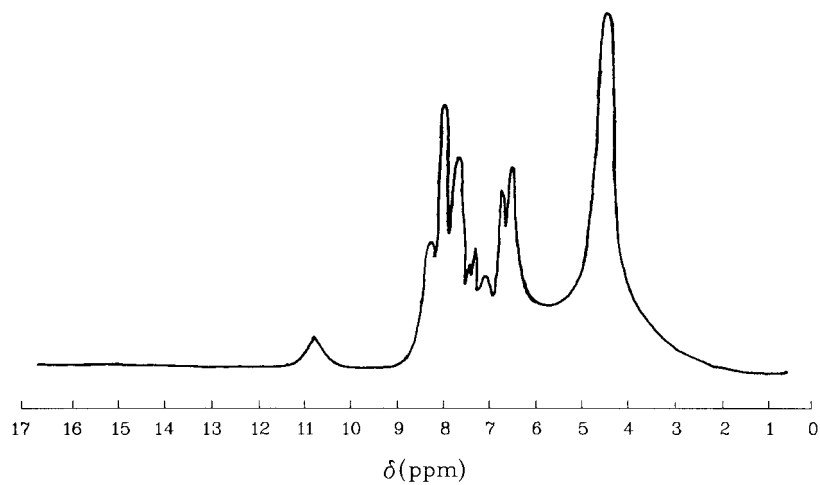
peak appears at 4.29 ppm, which may be caused

by exchange of the proton of —NH—— with  $\text{D}_2\text{O}$ . In Figure 3(b), the characteristic bands of amic acid disappeared, while the characteristic bands of imide ring at 1780, 1720, 1360, 1120, and 710  $\text{cm}^{-1}$  appeared. Therefore, a complete imidization was confirmed from the spectral changes.

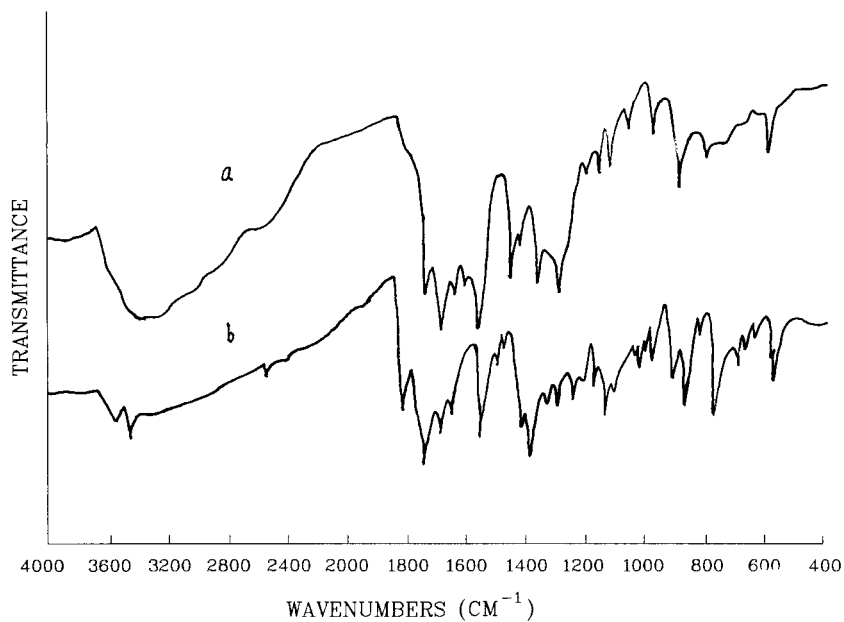
#### Thermal Properties

The TG-DTA curves of BTDA-PMDA APA1 and BTDA-PMDA API1 in air are shown in Figure 5. It can be seen that the curve of BTDA-PMDA APA1 can be divided into three stages: the first stage is associated with a slight weight loss resulting from the evaporation of the remaining solvent from ambient temperature to 106.8°C, with a small endothermic peak at 64.75°C; in the second stage, the TG curve shows a second slight weight loss at 146.8–221.8°C, and another endothermic peak at 168.8°C appeared in its DTA curve, which was considered to be related to the imidization; in the third stage, the TG curve gave a great weight loss above 502.3°C, owing to degradation via oxidation; meanwhile, two exothermic peaks at 537.6 and 599.4°C appeared in its DTA curve. For BTDA-PMDA API1, degradation didn't take place until 528.7°C. Its TG curve shows a marked weight loss, and its DTA curve has two exothermic peaks at 561.0 and 599.4°C.

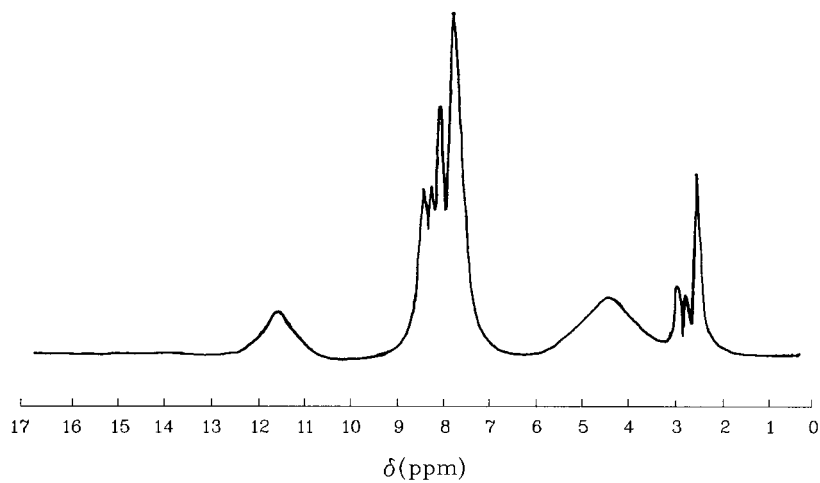
TG-DTA data of all BTDA-PMDA APA and BTDA-PMDA API are listed in Tables VIII and IX, respectively. It was found that all BTDA-PMDA APA have three-stages of thermal behaviors: evaporation of remaining solvent, thermal imidization, and thermal decomposition. And no thermal changes happened to BTDA-PMDA API before they began to undergo thermal decomposi-



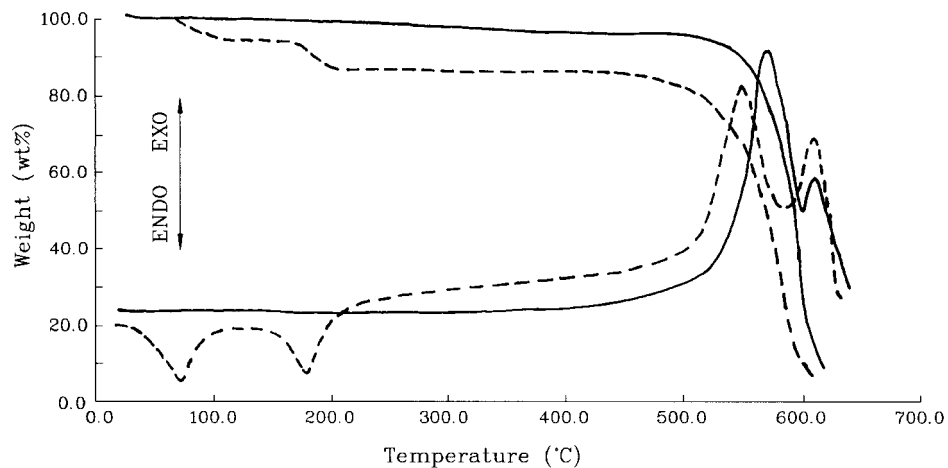
**Figure 2** <sup>1</sup>H-NMR spectrum of BTDA CED1.



**Figure 3** IR spectrum of (a) BTDA-PMDA APA1 and (b) BTDA-PMDA API1.


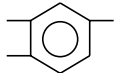


**Figure 4** <sup>1</sup>H-NMR spectrum of BTDA-PMDA APA1.



**Figure 5** TG-DTA curves of BTDA-PMDA APA1 (-----) and BTDA-PMDA API1 (—).

**Table IV**  $^1\text{H-NMR}$  Data of BTDA CED (ppm)

| Sample    | $-\text{CH}_2$ | $-\text{NH}_2/\text{D}_2\text{O}$ |  |  | $-\text{COOH}$ |
|-----------|----------------|-----------------------------------|---|---|----------------|
| BTDA CED1 | —              | 4.37                              | 7.39–6.50   | 8.18–7.67   | 10.74          |
| BTDA CED2 | —              | 4.80                              | 7.72–6.64   | 8.28–8.01   | 10.75          |
| BTDA CED3 | 3.72           | 4.83                              | 6.80–6.42   | 8.20–7.93   | 10.57          |
| BTDA CED4 | —              | 4.97                              | 7.64–7.05<br>6.71–6.61<br>7.65–6.82   | 8.21–7.99   | 10.56          |

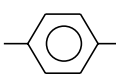
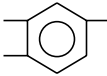
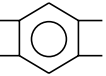
**Table V** Wavenumbers of BTDA-PMDA APA ( $\text{cm}^{-1}$ )

| Sample         | $-\text{COOH}$    | $-\text{NH}-\overset{\text{O}}{\parallel}{\text{C}}-$ | Phenyl Ring | Other Structure       |
|----------------|-------------------|---|-------------|-----------------------|
| BTDA-PMDA APA1 | 1710<br>3080–2700 | 3380–3200, 1655<br>1510, 1315                         | 1510, 1410  | —                     |
| BTDA-PMDA APA2 | 1710<br>3080–2700 | 3380–3200, 3650<br>1520, 1310                         | 1520, 1410  | —                     |
| BTDA-PMDA APA3 | 1720<br>3080–2700 | 3380–3200, 1630<br>1510, 1300                         | 1510, 1410  | —                     |
| BTDA-PMDA APA4 | 1710<br>3080–2700 | 3380–3210, 1640<br>1540, 1300                         | 1510, 1400  | 1220 ( $-\text{O}-$ ) |

**Table VI Wavenumbers of BTDA-PMDA API (cm<sup>-1</sup>)**

| Sample         | $\begin{array}{c} \text{O} \quad \text{O} \\ \parallel \quad \parallel \\ -\text{C}-\text{NH}-\text{C}- \end{array}$ | Phenyl Ring | Other Structure |
|----------------|--|-------------|-----------------|
| BTDA-PMDA API1 | 1780, 1720, 1360, 1120, 710  | 1510, 1360  |                 |
| BTDA-PMDA API2 | 1770, 1720, 1360, 1120, 700  | 1500, 1390  |                 |
| BTDA-PMDA API3 | 1780, 1720, 1370, 1130, 720  | 1500, 1370  |                 |
| BTDA-PMDA API4 | 1780, 1725, 1380, 1120, 720  | 1500, 1380  | 1250 (—O—)      |

**Table VII <sup>1</sup>H-NMR Data of BTDA-PMDA APA (ppm)**

| Sample         | CH <sub>2</sub> | $\begin{array}{c} \text{O} \\ \parallel \\ -\text{NH}-\text{C}-/\text{NH}_2/\text{D}_2\text{O} \end{array}$ |  |  |  | —COOH |
|----------------|-----------------|---|---|---|---|-------|
| BTDA-PMDA APA1 | —               | 4.29  | 7.68  | 8.23–8.00   |   | 10.66 |
| BTDA-PMDA APA2 | —               | 4.40  | 7.75–7.21   | 8.24–7.95   |   | 10.60 |
| BTDA-PMDA APA3 | <sup>a</sup>    | 4.07  | 7.61–7.20   | 8.24–7.92   |   | 10.65 |
| BTDA-PMDA APA4 | —               | 4.10  | 7.80–6.90   | 7.91–8.23   |   | 10.52 |

<sup>a</sup> Covered by the peak of  $\delta = 4.07$  ppm.

**Table VIII TG-DTA Data of BTDA-PMDA APA (°C)**

| Sample         | Volatilization Temperature |       | Imidization Temperature |       |       | Decomposition Temperature |        |        |
|----------------|----------------------------|-------|-------------------------|-------|-------|---------------------------|--------|--------|
|                | Peak                       | End   | Initial                 | Peak  | End   | Initial                   | Peak 1 | Peak 2 |
| BTDA-PMDA APA1 | 64.8                       | 106.8 | 146.8                   | 168.8 | 221.8 | 502.3                     | 537.6  | 599.4  |
| BTDA-PMDA APA2 | 52.7                       | 94.7  | 131.2                   | 165.5 | 212.4 | 505.1                     | 540.5  | 567.0  |
| BTDA-PMDA APA3 | —                          | 82.7  | 134.3                   | 156.1 | 199.8 | 496.5                     | 537.6  | 590.5  |
| BTDA-PMDA APA4 | 52.6                       | 88.6  | 143.6                   | 143.6 | 162.4 | 521.8                     | 531.8  | 550.3  |

All peak temperatures are from DTA, and all initial or end temperatures are from TG.

**Table IX TG-DTA Data of BTDA-PMDA API (°C)**

| Sample         | Decomposition Temperature <sup>a</sup> |        |        |
|----------------|--|--------|--------|
|                | Initial                                | Peak 1 | Peak 2 |
| BTDA-PMDA API1 | 528.7                                  | 561.0  | 599.4  |
| BTDA-PMDA API2 | 528.6                                  | 558.1  | 590.5  |
| BTDA-PMDA API3 | 467.3                                  | 581.9  | —      |
| BTDA-PMDA API4 | 502.3                                  | 534.6  | 602.3  |

<sup>a</sup> Temperatures of peaks 1 and 2 are obtained from DTA, and initial temperature is from TG.

**Table X TG-DTA Data of BTDA HPI and PMDA HPI (°C)**

| Sample    | Decomposition Temperature <sup>a</sup> |       |
|-----------|--|-------|
|           | Initial                                | Peak  |
| BTDA HPI1 | 543.5                                  | 578.8 |
| BTDA HPI2 | 567.0                                  | 590.5 |
| BTDA HPI3 | 520.0                                  | 543.5 |
| BTDA HPI4 | 543.5                                  | 552.2 |
| PMDA HPI1 | 531.8                                  | 567.0 |
| PMDA HPI2 | 531.8                                  | 555.0 |
| PMDA HPI3 | 542.0                                  | 583.0 |
| PMDA HPI4 | 538.0                                  | 550.0 |

<sup>a</sup> Initial and peak temperatures are from TG and DTA curves, respectively.

**Table XI Interfacial Tension Data of BTDA–PMDA API, BTDA HPI, and PMDA HPI**

| Sample         | Contact Angle<br>(degree) |            | Interfacial Tension<br>(dyne/cm) |              |            |
|----------------|---------------------------|------------|----------------------------------|--------------|------------|
|                | $\theta_1$                | $\theta_2$ | $\gamma_s^d$                     | $\gamma_s^p$ | $\gamma_s$ |
| BTDA–PMDA API1 | 90.0                      | 74.0       | 21.645                           | 8.329        | 29.974     |
| BTDA–PMDA API2 | 86.0                      | 74.8       | 17.379                           | 11.939       | 29.318     |
| BTDA–PMDA API3 | 84.5                      | 75.7       | 15.492                           | 13.634       | 29.176     |
| BTDA–PMDA API4 | 85.3                      | 74.3       | 17.335                           | 12.303       | 29.638     |
| BTDA HPI1      | 85.5                      | 72.3       | 19.436                           | 11.232       | 30.668     |
| BTDA HPI2      | 79.0                      | 70.2       | 16.774                           | 15.847       | 32.621     |
| BTDA HPI3      | 83.0                      | 70.3       | 19.440                           | 12.437       | 31.877     |
| BTDA HPI4      | 83.3                      | 73.1       | 17.023                           | 13.459       | 30.482     |
| PMDA HPI1      | 82.3                      | 72.0       | 17.337                           | 13.805       | 31.142     |
| PMDA HPI2      | 82.3                      | 70.3       | 18.916                           | 13.025       | 31.941     |
| PMDA HPI3      | 82.0                      | 70.7       | 18.323                           | 13.460       | 31.783     |
| PMDA HPI4      | 82.3                      | 72.0       | 17.337                           | 13.805       | 31.142     |

tion. Also, a small difference in the initial decomposition temperatures between a BTDA–PMDA APA and its corresponding BTDA–PMDA API was attributed to the different thermal imidization processes.

Table X gives the TG-DTA data of BTDA HPI and PMDA HPI. For the same diamines, the initial decomposition temperatures and the first exothermic peak temperatures of BTDA–PMDA API are found to be slightly lower than their corresponding homopolyimides (BTDA HPI or PMDA HPI).

### Interfacial Tension

Interfacial tension was worked out according to the harmonic mean method,<sup>10</sup> as follows.

$$\begin{aligned}
 (1 + \cos \theta_1)\gamma_1 &= 4[\gamma_1^d\gamma_s^d/(\gamma_1^d + \gamma_s^d) + \gamma_1^p\gamma_s^p/(\gamma_1^p + \gamma_s^p)] \\
 (1 + \cos \theta_2)\gamma_2 &= 4[\gamma_2^d\gamma_s^d/(\gamma_2^d + \gamma_s^d) + \gamma_2^p\gamma_s^p/(\gamma_2^p + \gamma_s^p)] \\
 \gamma_1 &= \gamma_1^d + \gamma_1^p \\
 \gamma_2 &= \gamma_2^d + \gamma_2^p \\
 \gamma_s &= \gamma_s^d + \gamma_s^p
 \end{aligned}$$

where superscripts  $p$  and  $d$  are the polar component and depolar component in interfacial tension, respectively; and  $\theta_1$  and  $\theta_2$  the contact angles

on the polyimide film by water and glycerin, respectively. At 25°C,  $\gamma_1 = 72.8$ ,  $\gamma_1^d = 22.6$ , and  $\gamma_1^p = 50.2$  dyne/cm;  $\gamma_2 = 63.4$ ,  $\gamma_2^d = 40.6$ , and  $\gamma_2^p = 22.8$  dyne/cm.

Interfacial tension data of BTDA–PMDA API, BTDA API, and PMDA API are listed in Table XI. For polyimides of  $p$ -phenyl diamine, the alternating polyimide had much lower  $\gamma_s^p$  and higher  $\gamma^d$  compared to the corresponding homopolyimides. As to polyimides of 4,4'-diaminodibenzene and 4,4'-diaminodiphenyl ether, the  $\gamma^p$  value of the homopolyimides is much higher than alternating polyimides. Much different from the above results, among polyimides of 4,4'-diaminodiphenyl methane, the  $\gamma^d$  value of alternating polyimide is approximately 3 dyne/cm higher than that of its corresponding homopolyimides. Furthermore, an interesting result is that all BTDA–PMDA API had interfacial tensions at 29–30 dyne/cm, being lower than those of their respective homopolyimides ( $\geq 30.48$  dyne/cm).

According to Wu,<sup>10</sup> interfaces of polymers with similar chemical structure have almost the same interfacial tension. From the aforementioned, we can see that the polar component  $\gamma_s^p$  and depolar component  $\gamma_s^d$  vary with different diamines and dianhydrides, but interfacial tension  $\gamma_s$  changed slightly. Our study showed that alternating condensation of polymerization cannot only adjust  $\gamma_s^d$  and  $\gamma_s^p$ , but also reduce  $\gamma_s$  markedly; thus, it may well be an effective way to modify polyimides.



## REFERENCES

1. M. T. Bogert and R. R. Renshaw, *J. Am. Chem. Soc.*, **30**, 1135 (1908).
2. G. M. Bower and L. W. Frost, *J. Polym. Sci.*, **A1**, 3135 (1963).
3. R. A. Meyers, *J. Polym. Sci.*, **A1**, **7**, 2757 (1969).
4. C. V. Avadhani, P. P. Wadgaonkar, and S. P. Vernekar, *J. Polym. Sci., Polym. Chem.*, **28**, 1681 (1990).
5. W. Zeng, W. Qiu, J. Liu, X. Yang, L. Lu, and X. Wang, *Polymer*, **36**, 3761 (1995).
6. W. Qiu, Y. Yang, X. Yang, L. Lu, and X. Wang, *J. Appl. Polym. Sci.*, **59**, 1437 (1996).
7. French Pat. 1,427,126 (1966) (to Dupont Co.)
8. N. A. Adrova, M. I. Bessonov, L. A. Laius, and A. P. Rudakov, *Polyimides*, Technomic, 1970, p. 163.
9. C. V. Avadhani and S. P. Vernekar, *Polym. Bull.*, **24**, 487 (1990).
10. S. Wu, *Polymer Interface and Adhension*, Marcel Dekker, New York, 1982.